

⁶ Langmuir, I. and Kingdon, K. H., "Thermionic Effects Caused by Vapors of Alkali Metals," *Proceedings of the Royal Society (London)*, Ser. A, Vol. 107, Jan. 1925, pp. 61-79.

⁷ Winograd, Y. Y., "On the Flow of Charged Particles in Accelerating-Decelerating Electric Fields," Sc.M. thesis, June 1964, Brown Univ.

⁸ Chen, F. F., *Plasma Diagnostic Techniques*, edited by R. H. Huddleston and S. L. Leonard, Academic Press, New York, 1965, pp. 113-117.

⁹ Tonks, L., Mott-Smith, H. M., Jr., and Langmuir, I., "Flow on Ions Through a Small Orifice in a Charged Plate," *The Physical Review*, Vol. 28, July 1926, pp. 104-128.

¹⁰ Chapman, S. and Ferraro, V. C. A., "A New Theory of Magnetic Storms," *Terrestrial Magnetism and Atmospheric Electricity*, Vol. 36, June 1931, pp. 77-97 and 171-186; Vol. 37, Dec. 1932, pp. 147-156 and 421-429; Vol. 38, June 1933, pp. 79-96; also "The Theory of the First Phase of a Geomagnetic Storm,"

Terrestrial Magnetism and Atmospheric Electricity, Vol. 45, Sept. 1940, pp. 245-268.

¹¹ Ferraro, V. C. A., "On the Theory of the First Phase of a Geomagnetic Storm: A New Illustrative Calculation Based on an Idealized (Plane not Cylindrical) Model Field Distribution," *Terrestrial Magnetism and Atmospheric Electricity*, Vol. 57, March 1952, pp. 15-49.

¹² Longmire, C. L., *Elementary Plasma Physics*, Interscience, New York, 1963, pp. 90-107.

¹³ Chapman, S., *Geophysics the Earth's Environment*, edited by C. Devitt, J. Hieblot, and A. Lebeau, Gordon and Breach, New York, 1963, pp. 373-502.

¹⁴ Lees, L., "The Interaction Between the Solar Wind and the Geomagnetic Cavity," *AIAA Journal*, Vol. 2, No. 9, Sept. 1964, pp. 1576-1582.

¹⁵ Petschek, H. E., "Magnetic Field Annihilation," Rept. 123, 1963, Avco Everett Research Lab., Everett, Mass.

AUGUST 1969

AIAA JOURNAL

VOL. 7, NO. 8

Plane Blast Wave Produced by "Dense Plasma Focus"

R. J. WOLF* AND Y. NAKAGAWA†

High Altitude Observatory, National Center for Atmospheric Research, Boulder, Colo.

A short coaxial electromagnetic accelerator with a fast-ringing energy bank has been used to produce a hot dense plasma. This plasma in turn is collected in a small diameter tube and used as a driver gas to produce plane stable current-free high Mach number shock fronts in the tube. These shocks closely resemble plane blast waves.

I. Introduction

A NUMBER of different modes of operation of a coaxial electromagnetic accelerator have been reported. In thermonuclear fusion research the accelerator has been used for the injection of a high kinetic energy plasma into magnetic confinement devices,^{1,2} and recently for the formation of a dense hot plasma near the front end of the center electrode (the phenomenon called the "dense plasma focus").³⁻⁵ The accelerator also has been used to produce shock waves⁶⁻⁸ in rarefied gases in aerodynamical applications. In this last application a dome-shaped shock front is usually formed⁷ due to the $1/r$ (where r is the radial distance) dependence of the magnetic field between the electrodes, and the shock front becomes unstable upon leaving the accelerator.^{6,8} Some studies of shock waves produced by the dense plasma focus have also been reported.^{9,10}

In this paper it is shown that if a coaxial accelerator is operated in a mode so as to form a dense plasma focus, then, by collecting this focused high-temperature dense plasma into a small tube, a plane stable current-free shock front can be obtained. It is further shown that the physical characteristics of this stable wave resemble closely a plane blast wave.

II. Experimental Arrangements

The schematic of the experiment is shown in Fig. 1. The coaxial accelerator (coaxial gun), consisting of two, 28-cm-

long, concentric copper cylinders of 8.25-cm and 4.75-cm diam was placed in a Pyrex glass tube of 10-cm diam. The accelerator was connected to the energy source, a condenser bank of six capacitors of total capacity 85 μf , with a low-inductance (11 nh) spark gap switch for each capacitor. The spark gap switch was operated in air at atmospheric pressure. A triggering system that provided negative trigger pulses was used for switching the gaps; the jitter in the switching of the six gaps was confined to less than 30 nanosec. The inductance of the circuit, excluding the accelerator, was 16.4 nh and the resistance was 1.2×10^{-3} ohms. The time required for the first quarter cycle of oscillation of the whole circuit (including accelerator) was 2.0 μsec .

A system of soft x-ray monitors placed near the front end of the accelerator was used to determine the temperature of the focused plasma. This system consisted of two photocells with absorber foils and was mounted on a vacuum-tight gimbal assembly; the gimbal system together with collimators provided the space resolution of the x-ray source to within 1 mm². With the use of different absorber foils, it was possible to determine the time-dependence behavior of the electron temperature of the focused dense plasma. In experiments, foils of 1.6 and 3.2 mg/cm² Al and 2.4 mg/cm² Be were used.

A Pyrex glass tube of 4-cm diam was placed along the axis 15 cm from the front end of the accelerator to collect the focused dense hot plasma. This tube was connected to a system that provided vacuum and the supply of hydrogen gas for experiment.

A 1.5-m dual grating spectrograph was used with photocells for the spectroscopic measurements in the visible range. The line emission of H β (4861 Å) of hydrogen atom and the continuum (5540-5550 Å), together with the line emission of Cu I (5218 Å), were monitored in experiments, and from these observations the temperature and density structures behind

Received August 28, 1968; revision received January 17, 1969. The authors wish to express their indebtedness to C. P. Wolfe for his technical assistance in the experiments and to G. C. Vlases for his many helpful suggestions.

* Research Assistant.

† Physicist.

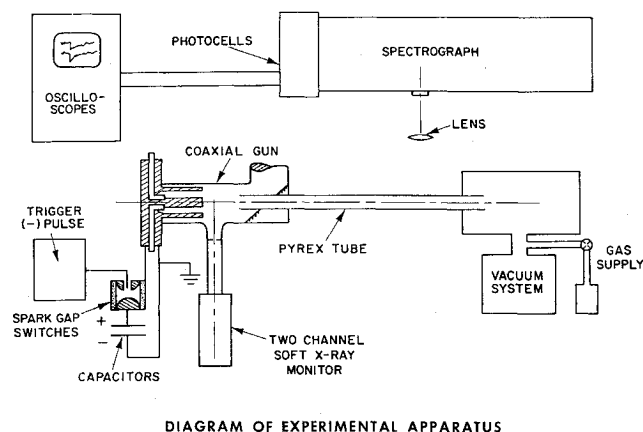


Fig. 1 Schematic arrangement of the experimental apparatus.

the shock front were determined; the line emission of Cu I was used to determine the position of copper plasma.

The azimuthal component of the magnetic field (B_θ) at various radial and axial locations downstream from the focus was measured with a seven-turn coil mounted on a 1.5-mm bobbin, which in turn was mounted on a long rod with a vacuum seal; the location of the coil could be varied without breaking vacuum. The response characteristics of the coil were carefully checked with a 5-Mc Helmholtz coil for signal distortion.

A piezoelectric probe,⁶ which utilized a 0.010-in.-thick Clevite PZT-4 crystal with a tin-lead alloy backing rod, was used for the pressure measurements. The diameter of this probe was 0.6 cm and its axis was always aligned parallel to the Pyrex tubes; thus, the response of this probe provided the relative amount of momentum flux (the sum of kinetic and hydrostatic pressures) in the axial direction. It was also possible to locate the probe at various positions without breaking the vacuum. Various streak and framing photographs of the luminous front were obtained with an image converter camera through a 100 Å half-band pass H_β filter.

III. Experimental Results

Experiments were performed with hydrogen gas of initial pressure 0.50 torr, and between each experiment the whole system was pumped down to 10^{-5} torr. In all experiments, the center electrode was kept initially at positive polarity and the capacitors were charged to 15 kv.

A. Formation of the Plasma Focus

If the accelerator and the external circuit are designed such that the current sheet arrives at the end of the electrodes near the time of peak current, the current sheet undergoes a very rapid radial collapse as it proceeds off the center electrode; this leads to the dense plasma focus.³⁻⁵ Figure 2a shows oscillograms of the soft x-ray monitor output from the region on the axis and 2 cm beyond the center electrode of the accelerator. Figure 2b represents the corresponding Rogowski coil pickup (dI/dt) and its integral (I) of the circuit oscillation. The discontinuity in the current corresponds to the collapse of the current sheet off the end of the center electrode.

The location and the time of formation of the dense plasma focus were determined by the use of the soft x-ray monitor. It was found that the dense plasma focus is formed in a volume along the central axis approximately 2 cm in length and $\frac{1}{2}$ cm in diameter located about 2 cm from the front end of the accelerator, and that the time of formation of the "plasma focus" (identified with the burst of x-ray emission) coincides

approximately with the time of maximum current in the accelerator circuit.

The maximum electron temperature of plasma in the focused region (defined by the x-ray burst of the longest time duration) was evaluated to be $(1.16 \pm 0.23) \times 10^6$ °K from the relative intensity of the x-ray emissions at different wavelengths measured by the x-ray monitor with the use of three different absorber films and the computations of Ref. 11. This estimate was based on the assumption that the observed x-ray emissions are resulting purely from hydrogenic Bremsstrahlung. The last assumption could be justified partly from the results of observation, since the ratio of any two of the three measurements yielded the same temperature (to within the estimated accuracy of the measurement). The presence of strong x-ray line or impurity emission would have resulted in excessive scatter in the temperature measured through the different absorbers. This assumption has been examined in greater detail in Ref. 5, and the existence of a Bremsstrahlung seems to be confirmed. The effects of impurity and line emission are discussed in detail in Ref. 11.

The electron number density within the focused region was estimated to be 4×10^{18} e/cm³ by applying a simple snow-pow theory, such that all the particles within the diameter of the center electrode were swept into the final measured diameter of $\frac{1}{2}$ cm of the focus. It is granted that this is a very rough estimate of the density; however, the density determined with this approximation is consistent with the measured densities and radii of collapse of Refs. 4 and 5. In addition, the attempt here is only to obtain an order-of-magnitude estimate of the total thermal energy content of the focused region so that it can later be compared to the energy required by plane blast-wave theory. Assuming an

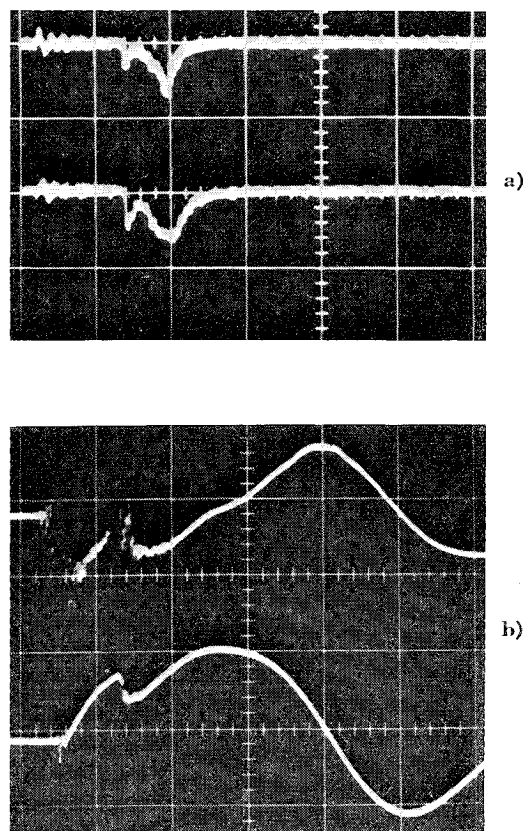


Fig. 2 a) Oscillogram of soft x-ray monitor output. Upper trace represents transmission through 2.4 mg/cm² Be absorber and lower through 1.6 mg/cm² Al absorber. b) Oscillogram of the circuit oscillation. Upper trace is the Rogowski coil output (dI/dt) and below its integral (I). The horizontal time scales are 2 μsec per division for both records.

ideal gas, the total thermal energy of the focused region can be estimated from $E_{th} = \frac{3}{2}NKT$, where N is the total number of particles in focused region and T their temperature. The total thermal energy was estimated to be 5×10^8 erg.

The focused region was also investigated by piezoelectric pressure probes. Measurements were made at 5, 10, and 15 cm from the front end of the center electrode and also at each 1-cm radial increment and of more than 200 independent firings of the accelerator. The axis of the probes was always parallel to that of the accelerator. Figure 3 represents a plot of the peak values of the pressure probe signals as a function of z and r . It can be seen that the axial momentum flux near the accelerator is also concentrated about a small diameter and diffuses radially as it progresses down the tube.

B. General Results With Small Tube

In order to collect the axial momentum flux (measured by the pressure probe) before its radial expansion, a small-diameter (4 cm) tube was introduced at 15 cm from the end of the accelerator (see Fig. 1). It was found that after the intersection of the current sheet and the small tube a plane stable luminous front is always formed and continues to travel in the small tube. Figure 4 illustrates framing camera photographs of the evolution of the shock front within the 4-cm-diam tube, and Fig. 5 is a streak photograph of the shock wave propagating inside the small tube.

It was found that the luminous front in the small tube remains plane and stable and that the magnetic probe signal was reduced by a factor of 10^{-3} in comparison with the similar signal taken at the same location without the small tube. Also, it was found that in the small tube the line emission of Cu I was reduced in amplitude and delayed considerably with respect to the H_β line emission; the latter remained practically unchanged with and without the small tube. Finally, the current-free nature of the wave in the small tube suggests that it could be identified with a blast wave resulting from the thermal expansion of the short-lived (1 μ sec) dense plasma focus.

C. Detail Analysis With Small Tube

Defining the shock front as the pressure discontinuity, determined by the pressure probe measurements, the ob-

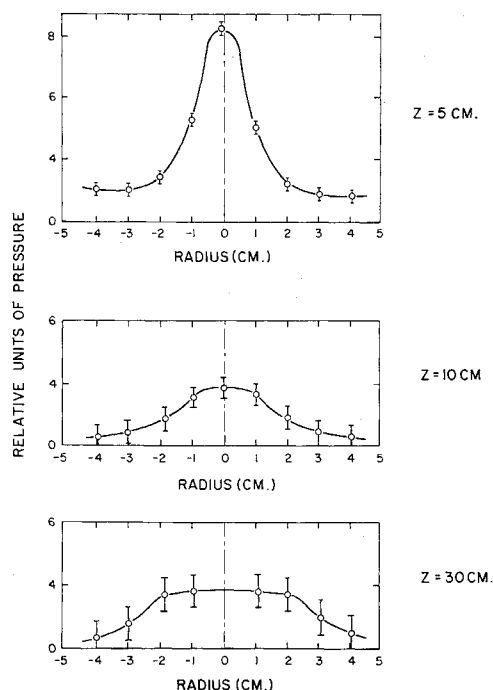


Fig. 3 Normalized hydrodynamic (hydrostatic and kinetic) pressure distributions at various distances Z from the accelerator.

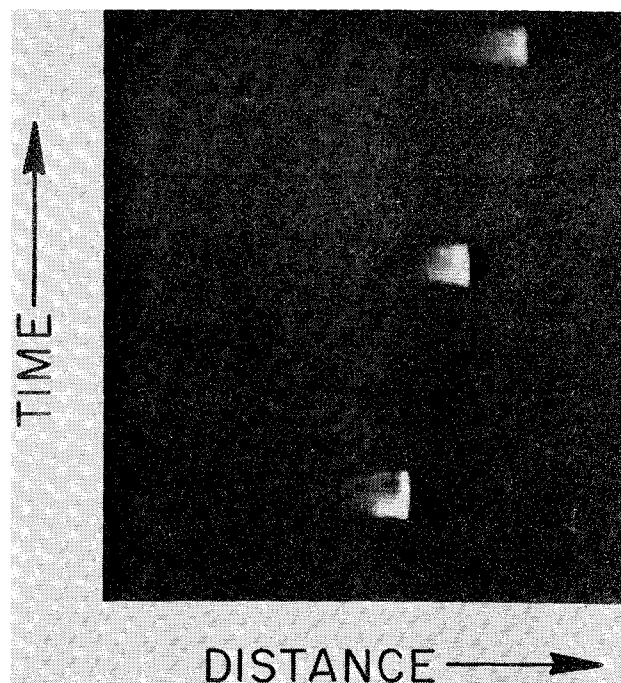


Fig. 4 Framing camera photographs of the shock-front evolution within the 4-cm-diam tube. The time increment is 0.5 μ sec between frames.

served trajectory is shown in Fig. 6. It was further found from detailed examinations of the oscillograms of pressure probe and H_β emission that there is practically no delay between onset of these signals; hence, the H_β luminous front in the small tube can also be identified as the shock front.

In order to confirm the blast-wave nature of the shock front inside the small tube, but to avoid complexity, a simple comparison of the observed shock trajectory with the similarity solution of plane blast wave was attempted. The

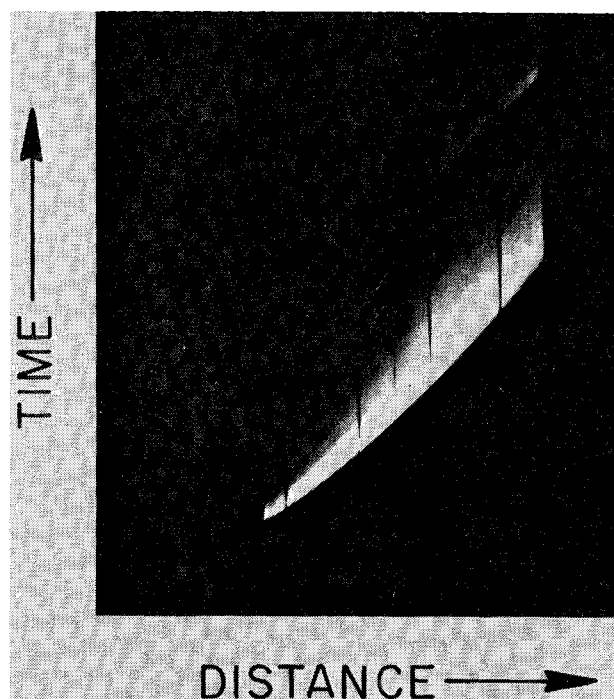


Fig. 5 A streak photograph of the front within the 4-cm-diam tube. Total streak duration is 20 μ sec, and the total field of view is approximately 50 cm.

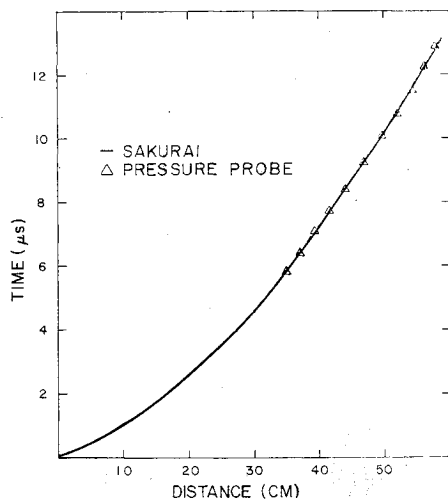


Fig. 6 Comparison of the trajectories of the pressure front (triangles) and the classical plane blast-wave similarity solution (solid curve).

classical similarity solution without chemical reaction for a plane blast wave can be written in the form, for $\gamma = 1.67$,^{12,13}

$$x_s = 0.853 (E_0/\rho_0)^{1/3} t^{2/3} \quad (1)$$

where x_s is the position of the shock front at time t , E_0 is the total energy released per unit cross-section area, and ρ_0 is the initial density.

The theoretical relation plotted in Fig. 6 was obtained after the least-squares fitting of Eq. (1) to the observed pressure-front data beyond the distance $z = 35$ cm from the accelerator. In constructing Fig. 6 and for the least-square fitting of Eq. (1), the position of the shock front x_s and time t were measured relative to the position and time of the maximum x-ray emission of the dense plasma focus. With the value of $E_0 = 4.72 \times 10^7$ erg/cm², a good agreement between the similarity solution and the experimental data has been obtained, as it can be seen in the figure. This implies that the 4-cm-diam tube collected a total energy of 5.9×10^8 ergs.

Further confirmations of the blast-wave nature of the shock front in the small tube were attempted by examining the density and temperature structure behind the shock front. This was done at seven locations, at 5-cm increments, starting from 35 cm and ending 65 cm from the focus. At 35 cm the shock Mach number is ~ 45 , the immediate postshock temperature $\sim 15,500^\circ\text{K}$, and the percent of ionization is $\sim 70\%$, while at a location 65 cm from the focus the shock Mach number is ~ 8 , the postshock temperature is $\sim 7,600^\circ\text{K}$, and the percent of ionization is $\sim 0.4\%$.

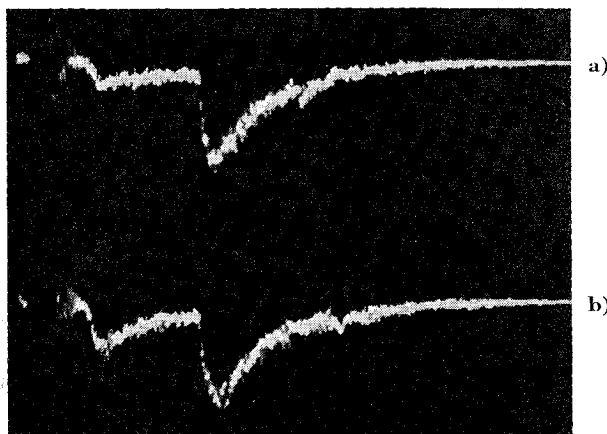


Fig. 7 a) H_β line emission intensity in a 10-Å interval about the line center and b) continuum emission intensity at (5540-5550 Å). The horizontal time scale is 5 $\mu\text{sec/div}$.

The temperature structure behind the shock was determined by the ratio of total H_β line intensity to the background continuum intensity (measured at 5540-5550 Å) utilizing the method described by Griem.¹⁴ Figure 7 illustrates H_β line and continuum emission intensities taken at a location 55 cm from the focus region. The conversion of temperature and density measured at several locations as a function of time to the nondimensional temperature and density (T/T_s and ρ/ρ_s , where T_s and ρ_s are the temperature and density at the shock front) as a function of the nondimensional parameter x/x_s (x_s being the position of the shock front) has been discussed by Vlasses and Jones.¹⁵ The present method of reducing the data, however, was somewhat different. The temperature was measured at one location (35 cm) x as a function of time t ; the position of the shock front x_s was measured simultaneously as a function of time (by a streak photograph); the dimensionless parameter $x/x_s(t)$ was then generated. The value of T_s as a function of time was measured at the following locations as the shock front arrived, producing $T_s(t)$.

Since at the shock front $x/x_s = T/T_s = 1$, the dimensionless function $T/T_s(t)$ and $x/x_s(t)$ could be generated. The time dependence of $T/T_s(t)$ and $x/x_s(t)$ was then eliminated to obtain T/T_s as a function of x/x_s only.

It should be noted that in the actual determination of the temperature and density behind the shock wave in the small tube, the intensity of H_β emission was measured through a 10-Å-wide slit. Thus, it was first necessary to compute the ratio of the total H_β emission, including the far wings, to the emission in a 10-Å interval about the line center. This was done as a function of electron temperature and density, employing the profiles computed by Griem.¹⁴

The temperature structure thus determined from these spectroscopic data is plotted in Fig. 8, together with the results of classical similarity solution in terms of nondimensional parameters T/T_s and x/x_s . The density structure determined from the absolute intensity of the H_β ¹⁴ emission with the assumption of Boltzmann distribution at the measured temperature was reduced in a similar fashion and is plotted in Fig. 9, in terms of nondimensional variables ρ/ρ_s (where ρ_s is the density at the shock front) and x/x_s with the results of classical similarity solution. It should be clear from these figures that the general physical characteristics of the observed plane stable shock front in the small tube closely resemble that of a plane blast wave.

The H_β line to continuum temperature measurement requires that equilibrium between the free electrons and third quantum level be attained and the result being representative of the electron temperature only. For the conditions of the experiment, this can be expected only for times greater than 0.1 μsec ¹⁴ or for values x/x_s less than 0.98 (see Fig. 8).

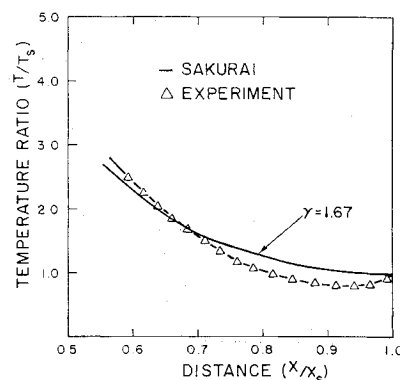


Fig. 8 Temperature structure behind the plane shock (triangles). Solid curve represents the classical plane blast-wave similarity solution for $\gamma = 1.67$.

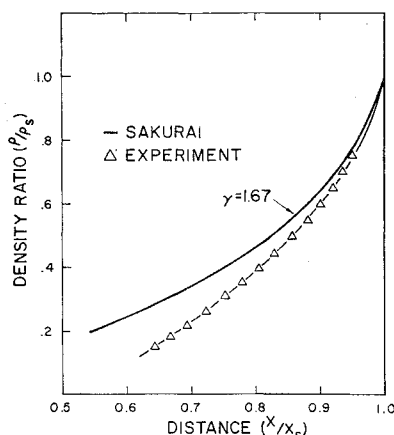


Fig. 9 Density structure behind the plane shock wave (triangles). Solid curve represents the classical plane blast-wave similarity solution for $\gamma = 1.67$.

The density measurement requires complete equilibrium between the electrons and the emitting hydrogen atoms. This can only be obtained for times greater than $3 \mu\text{sec}^{14}$ or for values x/x_s less than 0.95 (see Fig. 9). These conditions of nonequilibrium required that the values of temperature and density at the shock position x_s be extrapolated from data which were known to be in equilibrium.

IV. Concluding Remarks

In the present paper, the physical characteristics of shock waves produced by a coaxial accelerator are examined, and a method to produce a plane stable shock wave of high Mach numbers (up to 100 in hydrogen) with the use of a large energy fast-ringing accelerator is presented. It is shown that, by collecting the plasma from the region of dense plasma focus into a small tube, a plane stable shock wave can be obtained and that the shock wave resembles a plane blast wave. The exact physical nature of the shock wave will be the subject of future study.

It should also be noted that the value of $E_0 = 5.9 \times 10^8$ erg represents a collection of only $\frac{6}{10}$ of a percent (6.2×10^{-3}) of the original energy stored in the capacitor into the small tube. However, this value of E_0 represents the collection of possibly all the thermal energy of the dense plasma focus, which is approximately 5×10^8 erg and the additional kinetic energy of the plasma.

References

- ¹ Marshall, J., "Performance of a Hydromagnetic Plasma Gun," *The Physics of Fluids*, Vol. 3, No. 1, Jan.-Feb. 1960, pp. 134-135.
- ² Marshall, J. and Henins, I., "The Fast Plasma From a Gun," *Plasma Physics and Controlled Nuclear Fusion Research*, 1st ed., Vol. 2, International Atomic Energy Agency, Vienna, 1966, pp. 449-453.
- ³ Philippov, N. V., Philippova, T. I., and Vinogradov, V. P., "Dense, High-Temperature Plasma in a Non-cylindrical Z-pinch Compression," *Nuclear Fusion Supplement*, Pt. 2, 1962, pp. 577-583.
- ⁴ Mather, J. W., "Formation of a High-Density Deuterium Plasma Focus," *The Physics of Fluids*, Vol. 8, No. 2, Feb. 1965, pp. 366-377.
- ⁵ Mather, J. W. and Bottoms, P. J., "Characteristics of the Dense Plasma Focus Discharge," *The Physics of Fluids*, Vol. 11, No. 3, March 1968, pp. 611-618.
- ⁶ Chang, G. T., "Shock Wave Phenomena in Coaxial Plasma Guns," *The Physics of Fluids*, Vol. 4, No. 9, Sept. 1961, pp. 1085-1096.
- ⁷ Lovberg, R. H., "Schlieren Photography of a Coaxial Accelerator Discharge," *The Physics of Fluids*, Vol. 8, No. 1, Jan. 1965, pp. 177-185.
- ⁸ Koopman, D. W., "Performance Studies with an Electrically Driven Shock Tube," *The Physics of Fluids*, Vol. 7, No. 10, Oct. 1964, pp. 1651-1657.
- ⁹ Zhurin, V. V. and Suliaev, V. A., "Study of the Structure of Strong Shock Waves in Hydrogen and Helium," *Inzhenernyi Zhurnal*, Vol. 3, No. 4, pp. 645-657.
- ¹⁰ Belozarov, A., "Study of the Initial Ionization Process in a Strong Shock Wave," Rept. 131, June 1968, Univ. of Toronto Institute of Aerospace Studies, Toronto, Canada.
- ¹¹ Jahoda, F. C. et al., "Continuum Radiation in the X-Ray and Visible Regions from a Magnetically Compressed Plasma (Scylla)," *Physical Review*, Vol. 119, No. 3, Aug. 1960, pp. 843-856.
- ¹² Sakurai, A., "On the Propagation and Structure of the Blast Wave I," *Journal Physical Society Japan*, Vol. 8, No. 5, Sept.-Oct. 1953, pp. 622-669.
- ¹³ Sedov, L. I., "Problem of an Intense Explosion," *Similarity and Dimensional Methods in Mechanics*, 2nd ed., Vol. 1, Academic Press, New York, 1959, pp. 210-235.
- ¹⁴ Griem, H. R., "Temperature Measurements, Density Measurements, Equilibrium Relations," *Plasma Spectroscopy*, 1st ed., Vol. 1, McGraw-Hill, New York, 1964, pp. 279-281, 307-309, and 145-159.
- ¹⁵ Vlases, G. C. and Jones, D. L., "Experimental Study of Cylindrical Magnetohydrodynamic Blast Waves," *The Physics of Fluids*, Vol. 11, No. 5, May 1968, pp. 987-992.